We are IntechOpen, the world's leading publisher of Open Access books Built by scientists, for scientists

6,900
Open access books available

185,000
International authors and editors

200M
Downloads

Our authors are among the

154
Countries delivered to

TOP 1%
most cited scientists

12.2%
Contributors from top 500 universities

WEB OF SCIENCE™

Selection of our books indexed in the Book Citation Index in Web of Science™ Core Collection (BKCI)

Interested in publishing with us?
Contact book.department@intechopen.com

Numbers displayed above are based on latest data collected.
For more information visit www.intechopen.com

Chapter

The Mechanism of Misalignment of Saw Cutting Crack of Concrete Pavement

Chatarina Niken

Abstract

Misalignment cracks are transverse cracks that occur not in the cutting line but that are shifted within less than 500 mm of the cutting line. This crack does not cross other segments. This paper describes the mechanism of the formation of misalignment cracks and the stresses that occur in concrete pavement under plastic and brittle condition. This paper was written based on observations of misalignment cracks on toll roads in Lampung Province, Indonesia. Bending strength of the concrete pavement is ±4.5 MPa. This crack was found at the concrete age of 18–72 hours. This research is supported by observing deformation and inner temperature in the laboratory on a concrete plate with compressive strength of 60 MPa measuring 300 cm × 160 cm × 15 cm, which is placed on several supports. Observations were made every 15 minutes for 90 days. Misalignment cracks occur because cutting in concrete pavement is done in brittle conditions. Misalignment cracks were also found on one side, which dowel shift. In this phenomenon, misalignment cracks follow dowel shifting.

Keywords: concrete, crack, deformation, pavement, cutting, shrinkage

1. Introduction

Concrete or rigid pavement is often chosen as a road material that must withstand heavy loads. To withstand heavy loads, high-quality concrete is needed, which can only be made with limited water. The behavior of high-strength concrete has been studied [1, 2]. Apart from its ability, concrete pavement does not require expensive maintenance. Even with the best slab design and proper construction, however, it is unrealistic to expect crack-free and curl-free floor [3]. Humans, nature, and the type of the structural element affect the performance of concrete pavement forever.

Expansion and shrinkage naturally occur in the hydration process, due to, among others, product hydration growth, pore pressure, disjoining pressure, and surface force. It's called microprestress. It is easy to understand that microprestress always changes during time. Shrinkage and expansion are two behaviors that occur alternately in the concrete pavement. Concrete must be able to withstand these changes so that performance is good. There are many uncertainties to predict the shrinkage and expansion such as concrete composition, aggregate, relative humidity, and element structure geometry and ratio between open surface area and volume. Base course type also influences the concrete strength [4].

The concrete pavement has large surface contact to environment. Environment affects product hydration quality and drying shrinkage. Without covering the pavement right after pouring, inner water evaporates. Wind also accelerates inner water evaporation. This condition leads to the hydration process that occurs under limited water. It makes concrete more sensitive for premature cracks. More relative humidity is correlated to lower shrinkage [5]. The weather almost always has a role in the occurrence of uncontrolled cracking [6].

Hydration process results in heat that can reach 60°C [7]. A lot of concrete pores make the surrounding temperature to penetrate the concrete. Pouring fresh concrete during high surrounding temperature leads to the increase of the inner temperature. Heat evolution at any given time provides the change of mineralogical composition of the system [8]. An increase in equivalent linear temperature gradient leads to the increase in curvature for the unrestrained slab that was 7% higher than the restrained [9]. High inner temperature makes the hydration process occur with limited water. The consequence of this is premature deterioration and the change of expansion and shrinkage at early-age occur with high fluctuation.

Shrinkage is the root cause of random cracking in unreinforced concrete floors. From shrinkage to temperature, a large tensile strength in transversal direction on the bridge was studied [10]. Slow rate of shrinkage is a factor difficulty to predict the shrinkage accurately from laboratory measurement; therefore, minimum variant coefficient is assumed to be 20% to predict long-term shrinkage. Besides, this road has a dynamic problem. Compression and tension occur when the road is operational. The effect of shrinkage and creep was inserted by a solution for dynamic problem in reinforced concrete plate and beam [11].

Before applied load, microprestress occur in the concrete. Cracks can appear if no space is available for expansion and shrink. Open freely and joints help to release stresses. Joints of reinforced isolation were not as effective in reducing the edge stresses as compared to thickened joints [12]. The joints also help control unsightly transversal and longitudinal cracking, and also random slab cracking [13]. Cracks in joints are the consequence of concrete behavior in the initial period of use of pavement structures, which can affect structural properties of concrete pavements [14]. An overview of stress prediction for cracking of jointed plain concrete pavement was done in 1925–2000 [15].

Construction joint or contraction joint (also called control joint) can be made by open freely. Open freely make concrete pavement as unrestrained condition. Without joints, most concrete pavement would come in contact with cracks within 1 or 2 years after placement [16], except for continuously reinforced concrete (CRC) pavement, which has no joints. The open freely to be a place releasing the energy to avoid the premature and mature cracks. Open freely should be made in rigid pavement by saw cutting. While determining the location of the saw cutting, the distance where the shrinkage and expansion are still within the limits of the ability of concrete pavement must be considered. The depth of the saw cutting must really make this place the weakest location. Saw cutting must also consider the maturity of the concrete to be able to withstand microprestress at that age. Without those three things, we just move the location of the transverse crack. Late or shallow saw cutting of longitudinal joints causes longitudinal cracking [17]. Crack will shift from saw cutting line, hereinafter referred to as misalignment crack. Initial crack is not caused by misalignment of concrete pavement [18]. Vibration in the construction of concrete pavement in open traffic conditions makes the concrete pavement surface more at risk for the onset of hair cracks [7].

The inability of the concrete pavement to withstand all of the stresses can cause defects such as transverse and longitudinal cracking, cracks over dowel bars, cracks over slab culvert, blow up, crocodile cracks, hair cracks, etc. Road foundation (base/

subbase) settlement can cause a break in the rigid pavement or appear as a corner break depending on the location of the settlement. The cause of the crack must be understood in order to obtain the best concrete pavement performance.

These cracks and distresses do indicate the failure of concrete slab, but more than that, they indicate the human failure to understand the few basic and fundamental things related to concrete material and pavement. Implementers of concrete roads must have a sufficient understanding of the mechanism of the cracks in the concrete pavement to avoid the cracks. When it comes to the repair of distressed concrete pavement, very limited options are available. It is very difficult and time- and money consuming to repair hardened concrete [18]. Based on this statement, and limited analysis of misalignment crack, the mechanism of cracking needs to be studied and understood.

2. Plate deformation

2.1 Laboratory test specimen

Deformation of plate was found by full scale test in laboratory. The research was conducted in Jakarta, Indonesia, with humid tropical weather. This research was performed experimentally using one specimen of 3.000 × 1.600 × 150 mm^3, with four embedded vibrating wire strain gauges (EVWSG) as shown in **Figure 1a**. The plate was supported by many cylinders with 15 diameter and 30 cm high in horizontal position as shown in **Figure 1b**.

High-performance concrete with target compressive strength of 60 MPa and slump flow diameter of 35 ± 2 cm was applied. The plate was casted at 22.10 the night with surrounding temperature of 25.4°C and 94% relative humidity.

2.2 Laboratory observation of plate

In laboratory observation, shrinkage was measured as strain changes against time by installing four embedded vibrating wire strain gauge (EVWSG) in the specimen (**Figure 1a**). The EVWSG has abilities to detect the strain up to 3000 με with accuracy of about 0.025% and concrete temperature between −80°C and 60°C with about 0.5% accuracy. The specimens were covered with a plastic sheet to reduce evaporation of water immediately after casting. Observation was performed right after pouring as follows: (a). 0–24 hours, every 15 minutes; (b) 24–48 hours, every 60 minutes; and (c) 48–72 hours, every 2 hours. Relationship between strain and time and inner temperature and time were obtained.

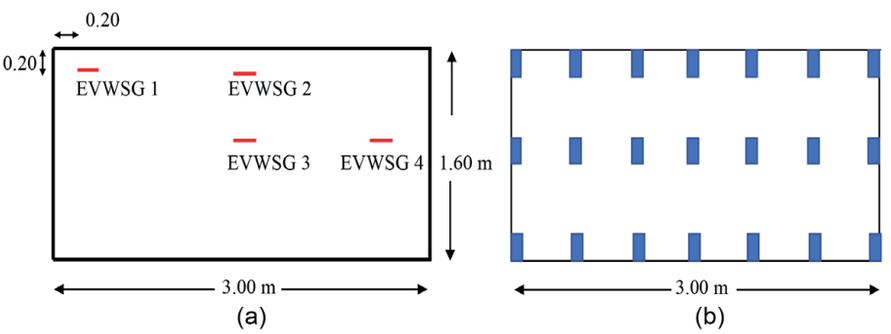

Figure 1.
The scheme of plate: (a) the placement of embedded vibrating wire strain gauges (EVWSG), (b) placement of plate supporter.

2.3 Relationship between deformation and time

Relationship between deformation of every position as shown in **Figure 1** during the first 90 hours was displayed in **Figure 2**.

Figure 2c shows that the highest deformation occurs in the middle of the plate, while the next sequence is in the corner of the plate (**Figure 2a**). The middle side of the elongated and shortened plates shows smaller deformation. Final concrete shrinkage in structure is about 600×10^{-6} [19]. Concrete capability to sustain tensile strain is about 600×10^{-6}. Cracks will appear if the shrinkage was restrained. Slab ≤4.5 m length will reduce tension stress. Slab with fc '60 MPa can shrink ±0.00022 mm/mm in the first 24 hours and at 1760 days of ±0.0003 mm/mm. Open freely is needed so that shrinkage can occur without obstacles. If there is no open freely, cracks will occur even though high-shrinkage cement is used.

2.4 Relationship between inner temperature and time

Inner temperature in early age shows a sharp increase in the age of 5–12 hours and then decreases gradually (**Figure 3**). The heat in concrete shows the activeness of the hydration process. The middle part of the plate shows the highest temperature, which is around 58°C (**Figure 3c**), while the angle is slightly below (**Figure 3a**). The middle side of the elongated and shortened side shows the peak of the lowest inner temperature, but it is still more than 50°C even though the concrete pavement is already 90 hours old and curing the humidity at the age of 24–168 hours (**Figure 3b** and **d**). At the age of 12–30 hours, there is a fairly large inner temperature gradient of ±28°C. Open freely is needed to release its energy. Open freely must be available before the concrete can hold the shrinkage energy. If there is a delay, a crack will occur. When curing the humidity is done, the inner temperature goes up to stabilize gradually until around 30° Celsius (**Figures 2** and **3**). It approaches the ambient air temperature, so the risk of cracking due to temperature difference decreases.

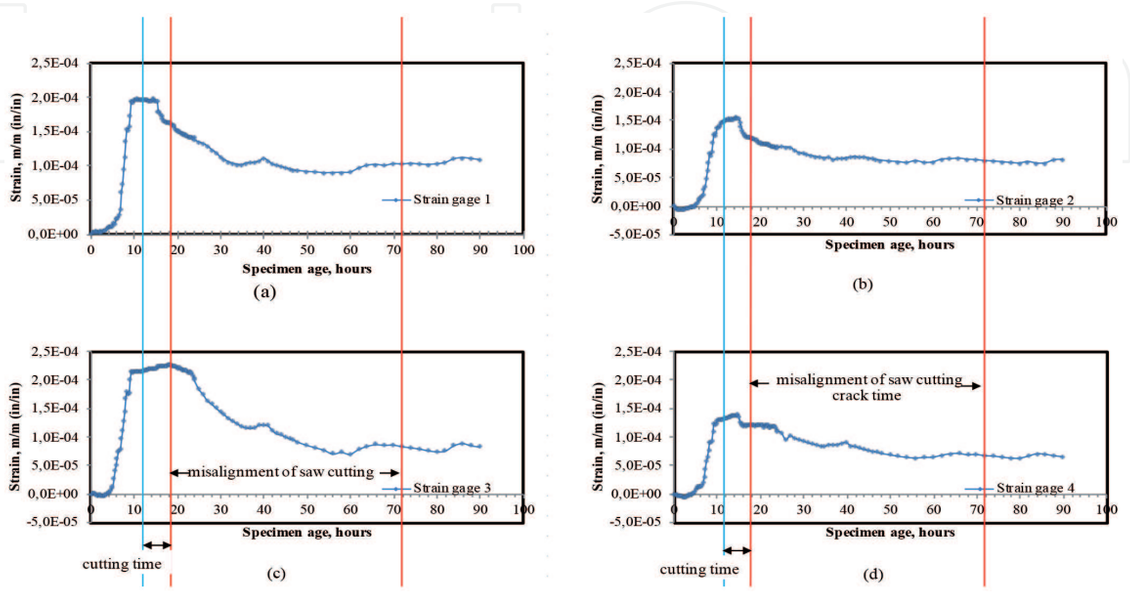

Figure 2.
Relationship between deformation and time of slab: (a) EVWSG 1, (b) EVWSG 2, (c) EVWSG 3, and (d) EVWSG 4.

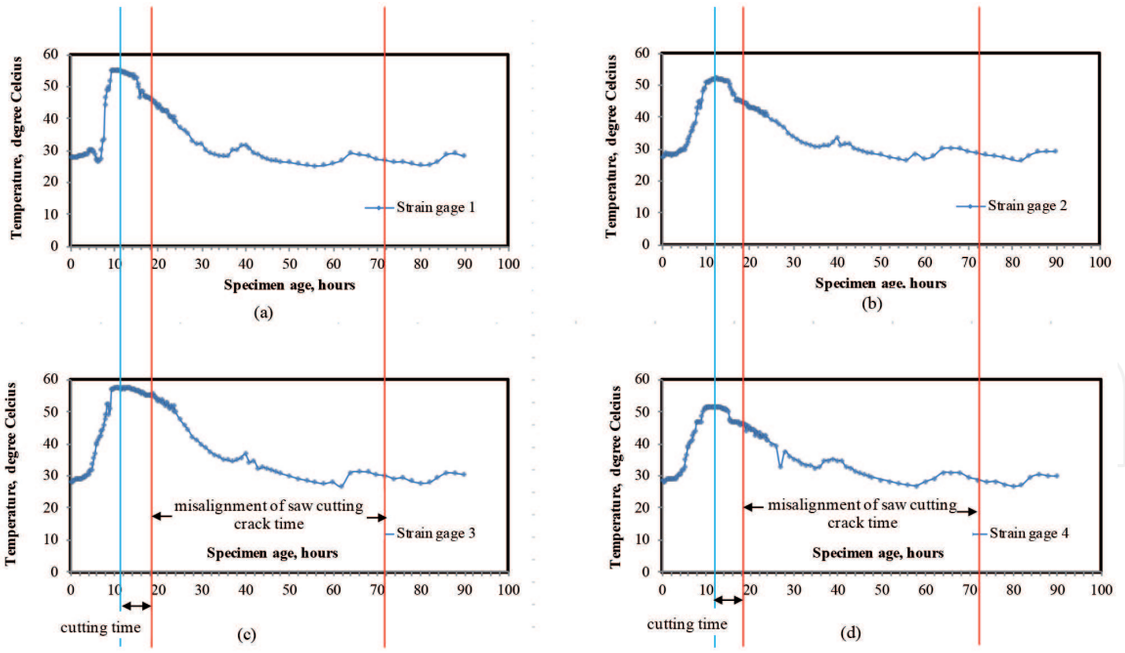

Figure 3.
Relationship between inner temperature and time of slab: (a) EVWSG 1, (b) EVWSG 2, (c) EVWSG 3, and (d) EVWSG.

According to the specification of the toll road, the cutting should be done in the time range of 12–18 hours that is when the rate of decline in the inner temperature is high (**Figure 3**). Cutting after this period results in misalignment cracks (**Figure 3**).

3. Concrete pavement

3.1 General over view

In this research, concrete pavement was done on the lean concrete plate. The aim of pouring on the plate is to sustain shear and tensile, which always appear under surface structure. Plate foundation can have different supported capacity [20].

The observation was done in the Bakauheni-Palembang road, Lampung Province, Indonesia, with 30,000 m length. The concrete pavement has four lanes (**Figure 4**). In this observation, the dowels have 32 mm diameter and 70 cm length, and the space between two dowels is 30 cm.

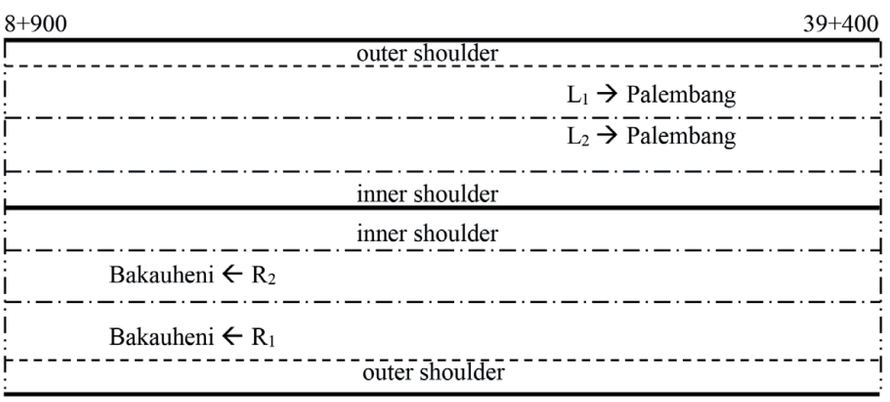

Figure 4.
Real concrete pavement scheme.

The lanes were divided into many segments. Each segment has 5 m length and 4.6 m wide; therefore, there are 600 segments for every lane or the total segments is 2400. Misalignment cracks appear in observation road (**Figure 5**).

A transverse crack in the middle of the span can cross the segment, but the misalignment crack does not cross to other segments. This happens because of different mechanisms of cracking. The types of defects observed that occur from 24,000 segments can be seen in **Table 1**.

Misalignment cracks are the second part of the three types of damage (**Table 1**). Eighty to ninety percent of the misalignment cracks occur on dowels that experience shifting or late cutting. The crack width is 1.5–2 cm with 30 cm depth or until the base of rigid pavement (**Figure 6**).

This damage is serious because it gets to the bottom of the concrete pavement. Understanding the mechanism of the occurrence of misalignment cracks is expected to trigger construction implementers to take preventative actions based on an understanding of the seriousness of the damage that will occur.

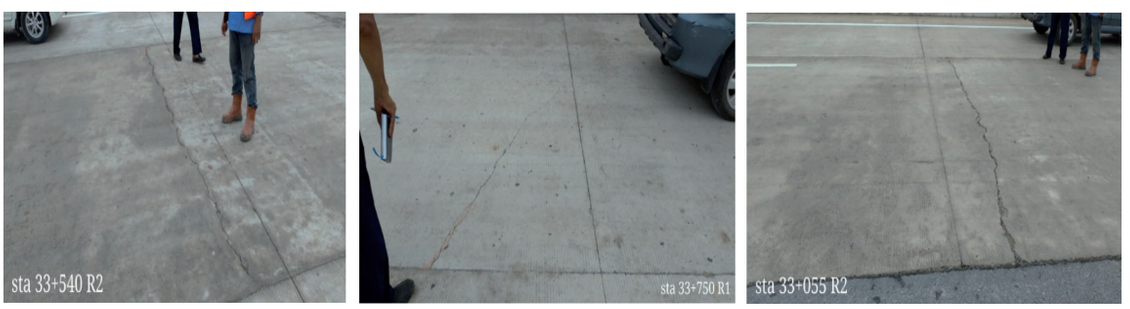

Figure 5.
Misalignment cracks: Bakauheni-Palembang.

Crack type	L segments	R segments	Total segments	% of total segments
Random	11	6	17	0.07
Misalignment	81	53	134	0.56
In the middle of the segment	98	94	192	0.8
Total			343	1.43

Table 1.
Percentage of crack type.

Figure 6.
Width and depth of misalignment crack.

3.2 Dowel

In general, concrete pavement is intended for heavy loads. To transfer the burden, dowels are required. Dowels made of plain reinforcement are installed between two segments (**Figure 7**).

The dowels were placed on the transversal bars, which formed as a chair (**Figure 8**). To maintain the chair and the dowel in the right position, some studs were placed by nailing it into lean concrete or LC (**Figure 8**). The dowel is mounted in the thick center of the rigid pavement (**Figure 9**). The lean concrete is 10 cm thick with compressive strength of 10 MPa (**Figure 9**). The rigid pavement has a bending strength of 45 MPa and is 30 cm thick. It was placed on the lean concrete covered with plastic membrant (**Figures 8** and **9**). A plastic membrant should be placed between the concrete/rigid pavement and lean concrete (**Figures 8** and **9**). The function of the plastic membrant was studied [7].

Pouring fresh concrete on the dowel should be done carefully, with little volume and slowly but continuously (**Figure 10**). This method is done to keep the dowel position still in right position. The dowel shift is caused by (1) the weakness of the stud installation so that it cannot hold the pouring of large volumes of fresh concrete at a location, or flattening and compaction by paver equipment (**Figure 10**) or (2) the weakness of binding dowel to basket.

When casting passes dowel line, the dowel position and its shift are recorded. Generally, the shifting dowel is between 10 and 20 cm from the correct axis (**Figure 11**).

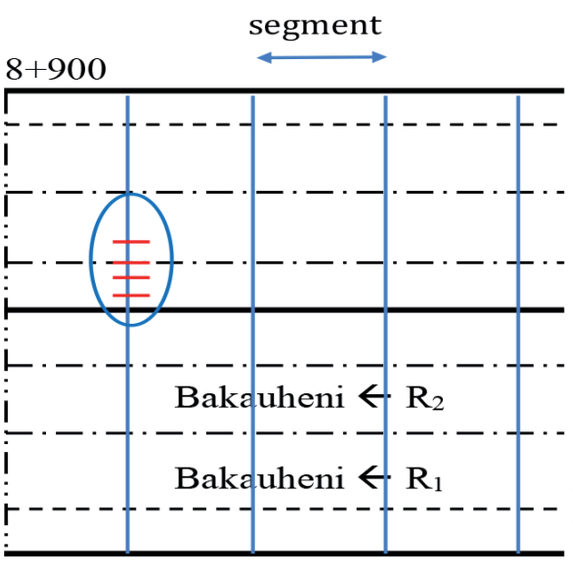

Figure 7.
Segment and dowel.

Figure 8.
Dowel baskets placed on an LC. Red line: Dowel. LC: Lean concrete.

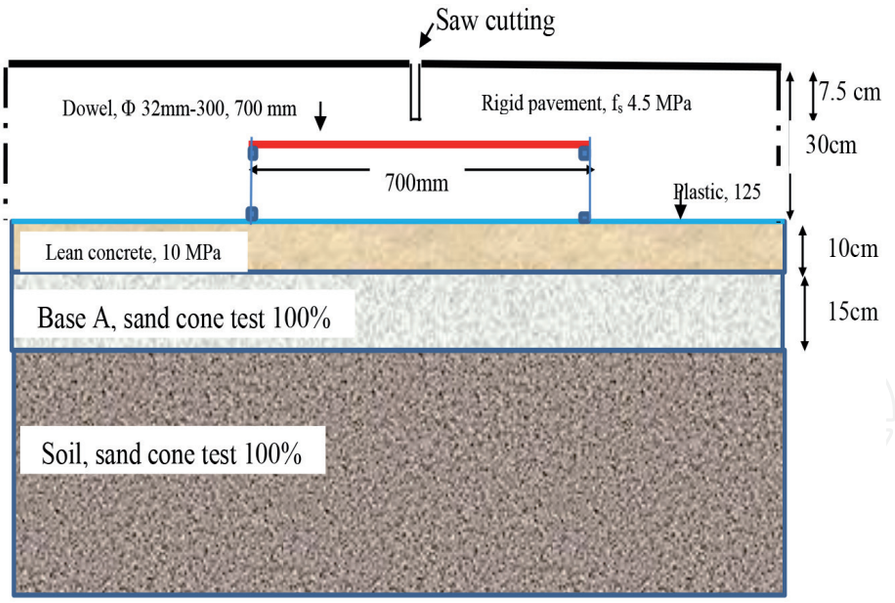

Figure 9.
Dowel position on cross-section.

Figure 10.
Pouring, flattening, and layering of the concrete/rigid pavement. Compaction process.

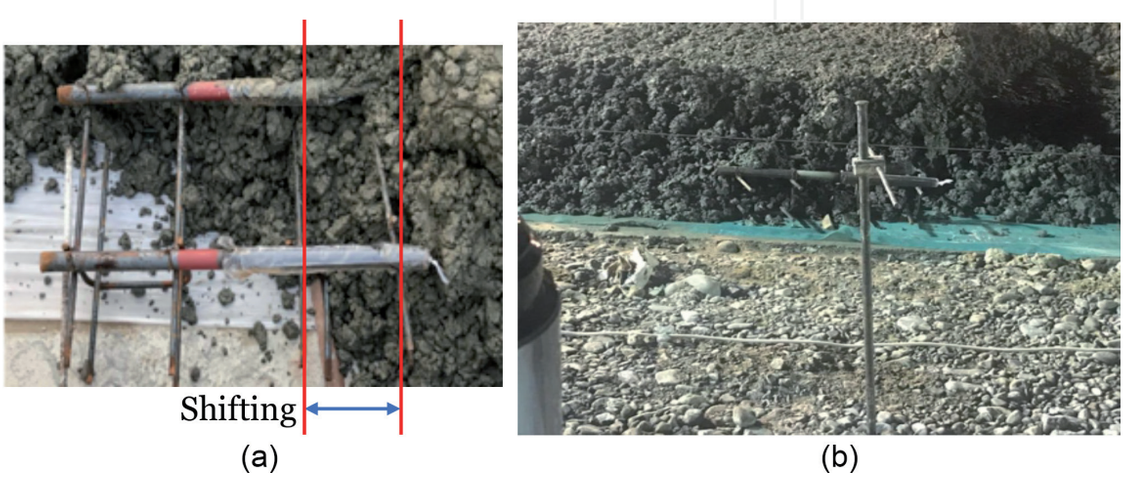

Figure 11.
Shifting dowel: (a) the top dowel holder shifts, and (b) the dowel holder shifts.

3.3 Saw cutting

Above the dowel line, a transverse cutting by saw is carried out, to direct the crack to occur at that place (**Figure 9**). Open free in concrete pavement by saw cutting means making the area weak. Cracking is planned to occur in the area (**Figure 12**).

If a crack exists below the saw cut, and an uncontrolled crack occurs nearby, then it is possible that dowels are misaligned and have caused locking of joint [18]. The depth of saw cutting varies, including D/2, D/3, and D/4. D is the thickness of rigid pavement. In this research, saw cutting was done above the as dowel line. The saw cutting depth d is D/4 (**Figure 13**). Cracks process and cracks area with various depths can be seen in **Figure 13a** and **b**.

Microcracking appears below the notch (**Figure 13a**). On cutting as deep as D/2, there is still a microcracking area that has not been covered (**Figure 13b$_1$**). This microcracking force will spread sideways and cause weakness in other areas. Whereas on cutting as deep as D/3, it can be said that undamaged areas are very thin (**Figure 13b$_2$**). On cutting as deep as D/4, the layer of area that protects against the distribution of microcracks is sufficient (**Figure 13b$_3$**). The distribution of concrete stresses under the saw cutting is as shown in **Figure 14**.

Concrete conditions when misalignment cracks are at the age of 18–72 are between plastic and brittle. Stress distribution at this time was assumed as shown in **Figure 14b** that is a transition between that shown in **Figure 14a** and **c**.

The stress distribution changes as the concrete maturity changes as shown in **Figure 15** [13]. Stress distribution as shown in **Figure 15** is distributed with cutting age 12 hours.

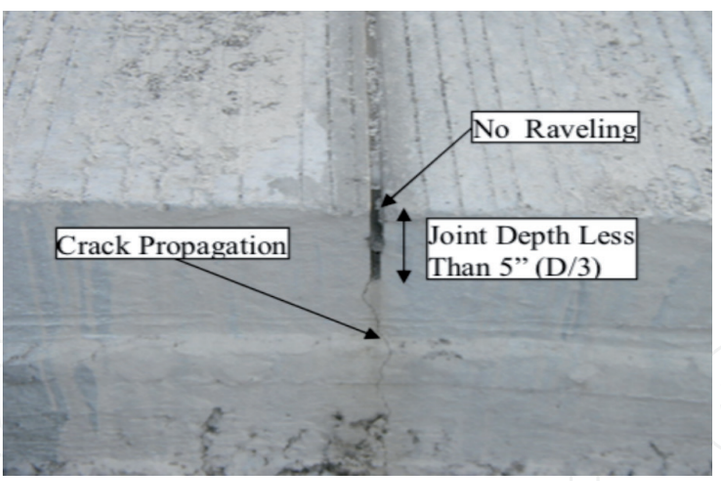

Figure 12.
Cracks occur at the planned place.

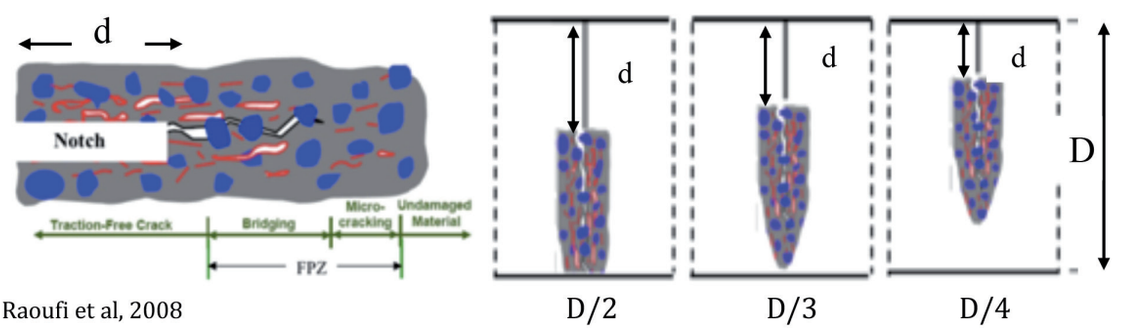

Raoufi et al, 2008

Figure 13.
Process and cracks area, (a) fracture process zone (FPZ), (b) FPZ in D/2, D/3, D/4 [13].

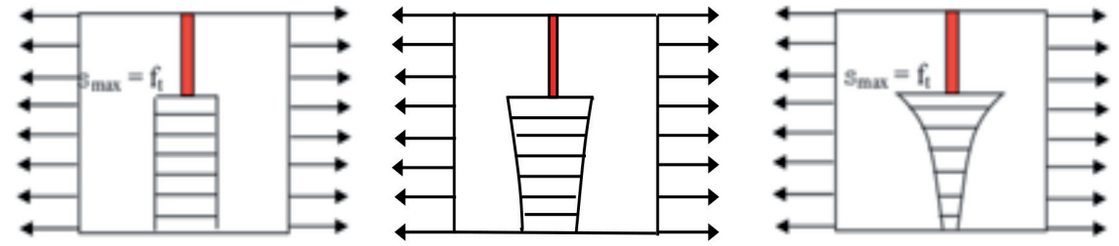

Raoufi et al, 2008 Raoufi et al, 2008

Figure 14.
Stress distribution: (a) plastic failure, (b) plastic-brittle failure, and (c) brittle failure [13].

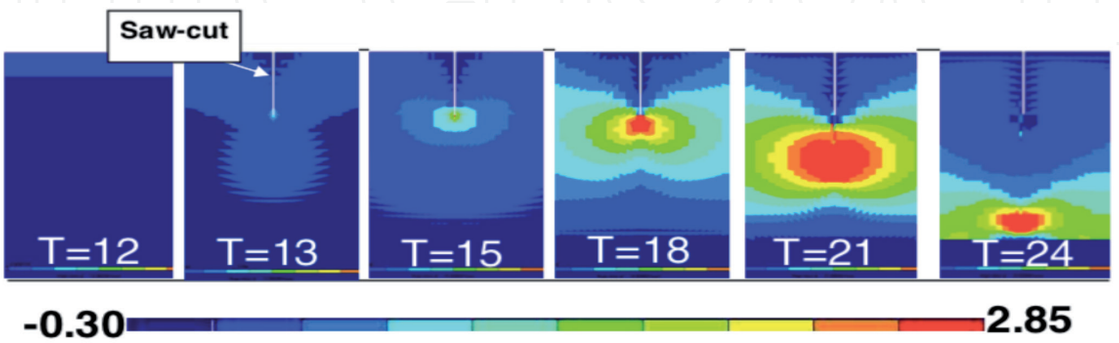

Figure 15.
Contour stresses at different times for rigid pavement with a D/3 cutting depth are carried out at 12 hours [13].

There is an optimum time to saw contraction joints in new concrete pavements, which is defined as the sawing window. It represents as short period after the placement of concrete within which concrete can be cut successfully before it cracks in an uncontrolled manner. If the sawing of the joints is started too early, then it may lead to raveling along the cut (**Figure 16a**). Concrete has not been able to withstand the pressure of the existing blade and microprestress. The jagged, rough edges are termed as raveling. Some raveling is acceptable if the widening of saw cut for filling joint sealant would remove the ravel edge. If the raveling is too severe, it will affect the appearance and ability to seal the joint. Saw cutting done at the beginning of the window time results in moderate raveling (**Figure 16b**) and at latter of cutting window time result good performance (**Figure 16c**). If sawing of joints is delayed beyond a certain period when significant concrete shrinkage occurs, then it may induce random cracks within the pavement.

Based on the results of the saw cutting, the appropriate time is at the end of the window time. Raoufi, 2008, [22] illustrates that excellent results will be obtained at fc '800–1000 psi (5.5–6.9 MPa). Saw cutting on rigid pavement according to the specification of this research should be done in the time range of 5–18 hours. At this age, the shrinkage begins to change into expansion (**Figure 2**) and the temperature inside the concrete has reached a maximum value (**Figure 3**). High temperatures cause the particles to move fast, resulting in collisions between molecules. This

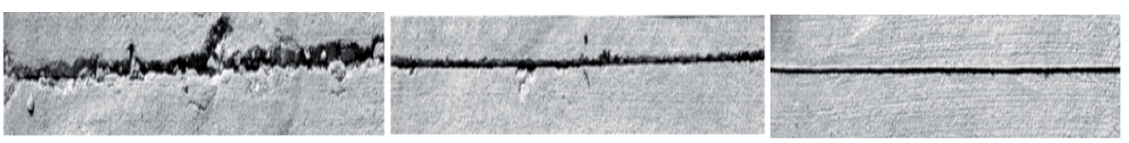

(a) (b) (c)

Figure 16.
Saw cutting result: (a) sawed too early (unacceptable), (b) sawed early in window (moderate), (c) sawed latter in window (acceptable) [21].

impact energy requires a place to release so there is no build-up. With saw cutting done in the window time, there is a space for expansion and shrinkage, so that cracking does not occur anywhere else. Notch from saw cutting is also a place for releasing energy.

Misalignment cracks as shown in **Figure 5** appear at the age of 18–72 hours. The crack follows the location of the shifted axle. Distance of the crack is about 50 cm from cutting line axle. Theoretical and practical studies have shown that the optimum joint spacing depends upon the slab thickness, concrete aggregate, subbase, and climate. Pavement with long transverse joint spacing may crack at locations other than the saw cuts due to tensile stresses from temperature curling. Most of the time, the spacing of transverse contraction joints in plain pavement is kept at 4.5–6.0 m. It is also important to check the transverse and longitudinal contraction joint spacing to see if it is within the limit as described in various codes and specifications. Saw cut transverse joint at proper location with respect to position of dowel bar assembly is a common construction practice. But some occasional mistakes may happen resulting in the misplaced saw cut. Proper location of saw cut dowel assembly not only improves the joint load transfer efficiency but also ensures better performance of the pavement throughout its life. Tolerance for sawing transfer joint, that is, the allowable translation of saw cut from the middle of the dowel assembly, depends upon the length of the dowel. It has been found that 15 cm of dowel embedment is all that is necessary for an effective load transfer under highway loadings. Thus, for a commonly used 50 cm long dowel bar, the available tolerance is 20 cm, that is, 10 cm either way from the center of the dowels.

4. Misalignment crack mechanism

To analyze the mechanism of crack misalignment, the influence of growth of hydration, decreasing pores, and microprestress needs to be understood.

4.1 Growth of product hydration and decreasing pores

The amounts of pores and the growth of product hydration can be seen in **Figure 17** [23]. t_c is the misalignment cutting time crack in the observed toll road.

The time frame for the appearance of misalignment cracks is expressed as t_c in **Figure 17**. During this time, the rate of hydration products' growth such as CSH, CH, C-A, F-H is very high; ettringite reaches its maximum and then decreases because part of it turns into monosulfate; and the number of pores decreases at a high rate.

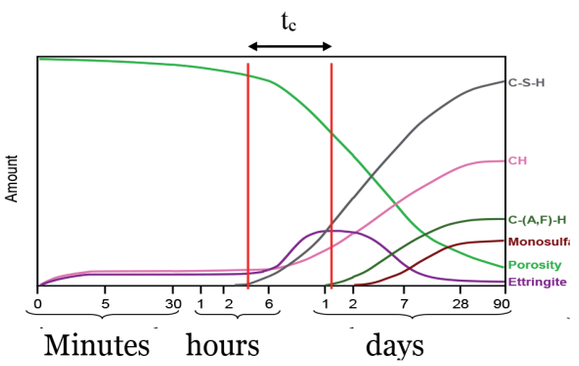

Figure 17.
Product hydration growth and decreasing pores.

4.2 Microprestress

Product hydration growth and decreasing pores cause stress in the concrete. The microstress is known as microprestress. Microprestress is the stress in micromeasurement, which occurs without applied load. Microstresses are due to the growth of hydration products, capillary pore pressure, disjoining pressure, and surface pressure [24]. Stress due to heat hydration, shear between fresh concrete and lean concrete, and shear between concrete and dowel are also classified as microprestress. Misalignment cracks in the concrete pavement occur at 18–72 hours (**Figure 17**). In that time span, the strain and temperature of the concrete decrease gradually (**Figures 2** and **3**). The growth rate of hydration products and the decrease of pore number rate in the span of time are very high (**Figure 17**). The consequence of this is that high stress occurs in the concrete matrix and in the pores (**Figure 18c**). This period is a critical time after the autogenous phase. Beside the microprestress, Buchta, 2015, [20] mentioned that the shear and tensile were concentrated on the base of the plate. This phenomenon will increase the microprestress. This is because the strain in the center of the plate is higher than in the surrounding area (**Figure 2**). The causes of microprestress will be explained below.

4.2.1 Product hydration growth pressure

The hydration process makes fresh concrete evolve into hard concrete (**Figure 18a** and **b**).

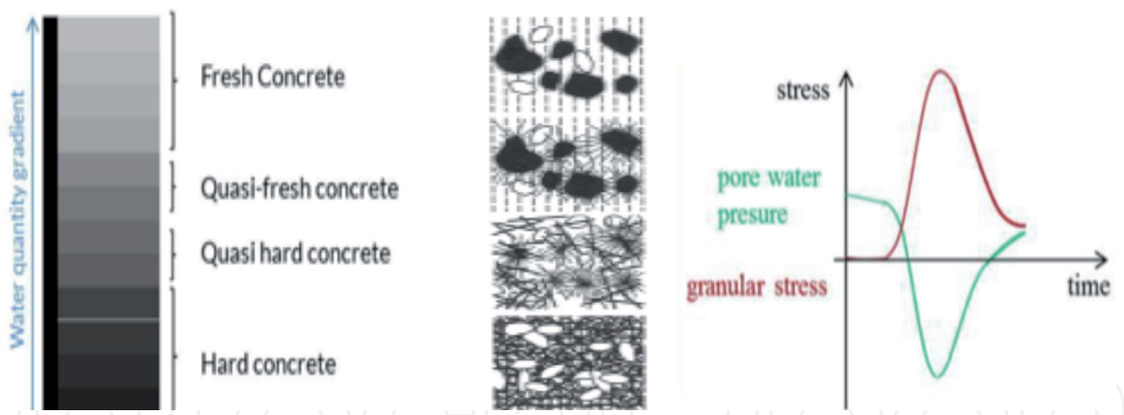

Figure 18.
Concrete evolution, (a) water quantity gradient, (b) microstructure evolution, (c) granular stress and pore water pressure [23, 25].

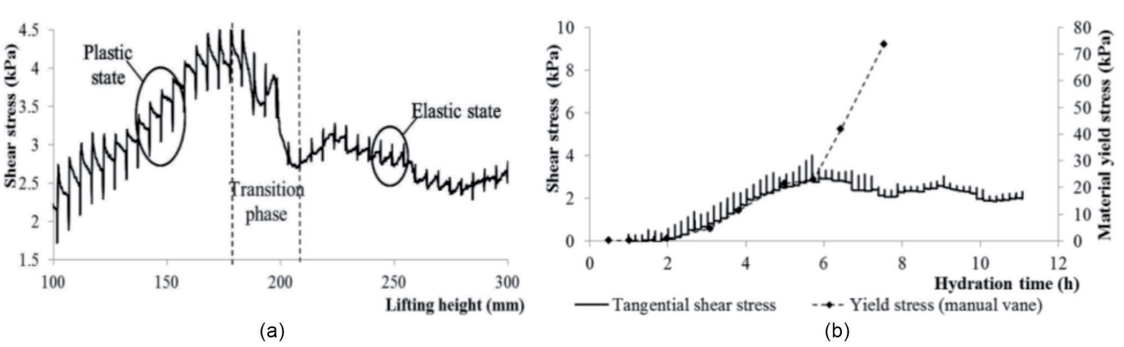

Figure 19.
Mortar behavior evolution: (a) behavior type, (b) material yielding [25].

Quasi hard concrete occurs after the age of 6 hours when the CSH growth rate increases (**Figures 17** and **18a**) and yield stress occurs (**Figure 19b**). The characteristic of quasi-brittle material is a strong nonstatistical size effect on both the structural strength and the rate of shrinkage and creep [25].

This evolution changes the deformation behavior of plastic behavior into a phase transition, and then changes to elastic state (**Figure 19a**). The behavior of microprestress in mortar or concrete also changes; at first microprestress is able to penetrate water at fresh and quasi-fresh concrete and then turn into bouncy due to hitting the quasi-hard and hardened concrete and also reinforces bar and dowel (**Figure 18a** and **b**). The bouncy power can break the weak bond and microcrack occurs. Concrete such as quasi-brittle structures fails at the macrocrack initiation, which can appear from the microcrack growth. Shear coefficient was also changed due to the increase of the concrete hardness and the power of microprestress. The change of shear stress can be seen in **Figure 19b**. The change from plastic state to transition phase is mentioned by Craipeau et al., 2018, as yield stress (**Figure 19b**) [25]. Concrete yield stress according to **Figure 19b** is about 22 kPa (0.022 Mpa) and occurs at the age of 6 hours. At the concrete age of 6 hours, C-S-H and ettringite begin to grow rapidly (**Figure 17**). If the dot line (**Figure 19b**) is continued, in the range of 18–72 hours, the shear stress is 320–1914.3 kPa (0.32–1.9 MPa).

Granular stress and pore water pressure show a similar value (**Figure 18c**). If it happens together, it will negate each other.

4.2.2 Evaporation

Evaporation occurs immediately after placement until the sample is tightly closed. Slowik et al., 2013, [26] found that although the rigid pavement was done by curing agent, evaporation still occurred (**Figure 20**).

In the first 30 minutes, there was a similarity of evaporation water between with and without curing, which is ±0.35 kg/m^2 (**Figure 20**). Evaporation without curing at 360 minutes (6 hours) is about 2.7 kg/m^2 or 2.7 10^{-6} MPa. Evaporation charts tend to be asymptotic after 360 hours (**Figure 20**); thus, evaporation at 3 days can be approached with 3 kg/m^2 or 3. 10^{-6} MPa without curing condition. This value was chosen because it shows the highest risk.

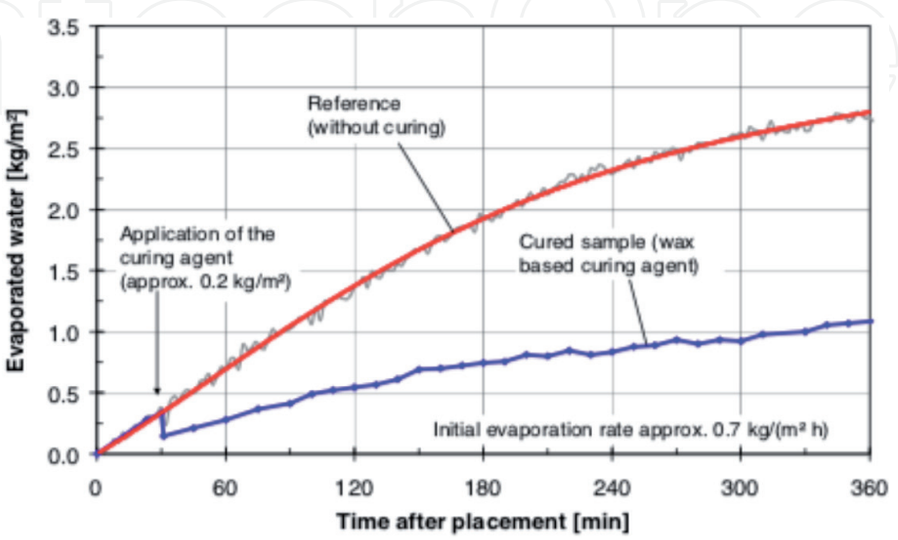

Figure 20.
Evaporation [9].

4.2.3 Capillary pressure

Water in the capillary pores causes tension pressure. Capillary pressure occurs quickly in concrete that contains more cement and less water (**Figure 21**).

By assuming that the capillary stress continues to run linearly, from **Figure 21b**, a capillary stress was obtained of approximately 163–828 kPa or 0.163–0.828 MPa in the age range of 18–72 hours. This figure is an estimate due to the influence of relative humidity.

The size and number of pores change due to the hydration process (**Figure 17**); therefore, capillary tension always occurs. The larger pores will dry and smaller pores will remain saturated. The surrounding relative humidity affects pore size (**Table 2**).

Because the surrounding relative humidity (RH) always changes, so does the capillary stress. Pore size determines the ability of water evaporation, menisci strength, and its properties. Pores with smaller sizes indicate that the smaller the evaporation ability, the smaller the evaporation stress [28]. Medium capillary pores (50–10 nm) and small gel pores (10–2.5 nm) have strong menisci [28]. The strong menisci mean strong capillary pores.

4.2.4 Disjoining pressure

Disjoining pressure is a pressure due to the attractive force between two surfaces, divided by the area of the surfaces; thus, disjoining pressure depends on the distance between the two surfaces. Correlation between inner water thickness and disjoining pressure was presented by Peng et al., 2015, as shown in **Figure 22** [30]. The thicker the inner water, the smaller the disjoining pressure. Maximum disjoining pressure is 50 bar (**Figure 22a**) or 5 MPa.

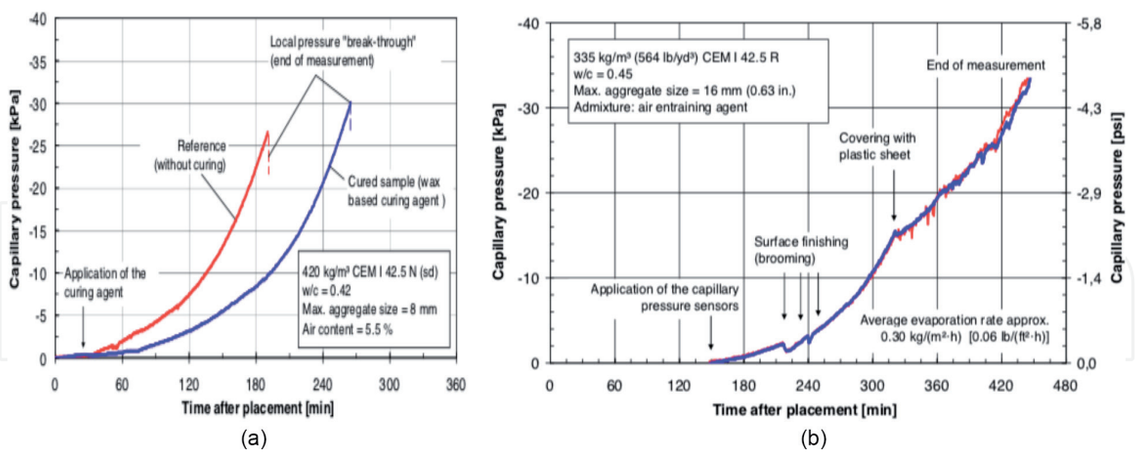

Figure 21.
Capillary pressure: (a) 420 kg/m², w/c 0.42; and (b) 335 kg/m², w/c 0.45 [27]. Source: Slowik et al. [22].

Relative humidity	85%	74%	54%	33%	<33%
Pore diameter (mm)	13	7.8	3.4	~1	<1
Origin of pores	Capillary pores	LD C-S-H (gel pores)		HD C-S-H	C-S-H structure

Source: Jenning et al., 2005 [18].

Table 2.
Theoretical relationship between relative humidity and pore size.

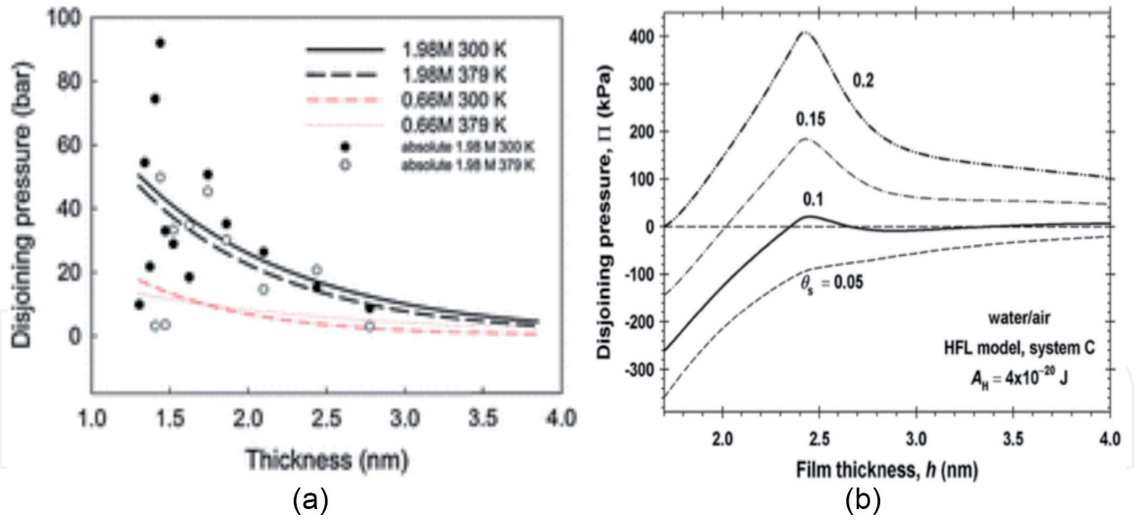

Figure 22.
Disjoining pressure: (a) disjoining pressure of water, and (b) total disjoining pressure for foam films and for the surfactant [4, 29].

4.2.5 Total microprestress

Total microprestress is taken from the description above. The values above are approach values not absolute values; it happens because there is evolution in the concrete that always occurs, and the influence of surrounding relative humidity makes microprestress to be always changing. The highest risk is anticipated by selecting extreme values from the description above (**Table 3**).

4.3 Dowel effect

There is friction force between dowel and concrete. The friction is not constant because the microstructure of concrete has evolved over time. Friction of steel in fresh concrete was observed [27]. Rabbat and Russel, 1985, have studied friction coefficient of steel on concrete or grout [10]. The effect of dowel on misalignment crack is divided into cutting at window time and cutting at out of window time with dowel in right position and shift position.

4.3.1 Cutting at window time

4.3.1.1 Dowel in right position

Placement of the correct dowel position and sawed in window cutting time result a crack occurring right in the saw cutting line (**Figure 12**). When saw

Type of microprestress cause	**Maximum pressure, MPa**
Product hydration growth	1.9
Evaporation	3.10^{-6}
Capillary pressure	0.83
Disjoining pressure	5
Total	7.730003

Table 3.
Maximum stresses from various causes of microprestress.

cutting is done, the frictional force between the dowel and concrete is balanced on both sides of the saw cutting line, penetrating the fracture that occurs and creeping. Microprestress penetrates cracks and then propagates under rigid pavement. Propagation of these forces in the area under the saw cutting increases the high stress that is collected at the lower end of the saw cutting line. This makes the saw cutting line the weakest area, so cracking occurs in the area (**Figure 23**).

4.3.1.2 Dowel in shift position

Dowel can shift from the right position (**Figure 11**) due to the pounding of fresh concrete pouring or because it is displaced by a paver (**Figure 10**). Naturally, there are shear force between dowel and concrete. Shifting dowel makes unbalanced shear force between both sides of the cutting line. Addition with microprestress and concentrated stress at the lower end of the saw cutting separates unevenly due to the dowel shift and increases unbalanced stress on both the sides. To be balanced, then when cutting arises the pulling force of restraint (**Figure 24a**). The consequence of this is that cracking does not occur in the cutting line but shifts at the starting point of the holding force.

The microprestress can reach 2.73 MPa as in item 4.2.5; if added dowel frictional force and stress concentrated at the lower end of the notch can exceed the strength of concrete that is 5.5–6.9 MPa (point 3.3). This can cause microcracks to arise in the concrete. The microcracks and high stress at one side of the cutting line lead to misalignment cracks (**Figure 24b**).

4.3.2 Cutting at out of window time

Saw cutting is done after the plastic period in which stress distribution is approached as shown **Figure 14b** and enters brittle condition. The brittle

Figure 23.
Dowel in right position: (a) shear stress between dowel and concrete and right crack, (b) cross crack in right position.

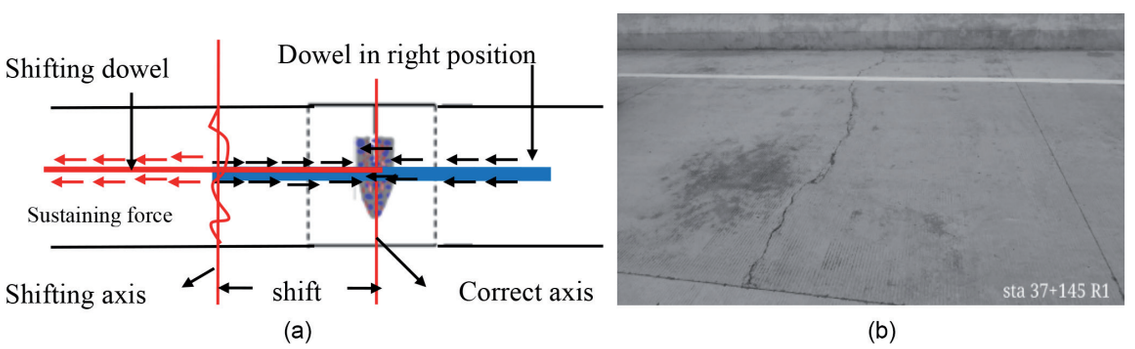

Figure 24.
Dowel in shift position: (a) shifting dowel and unbalanced stress, (b) misalignment crack.

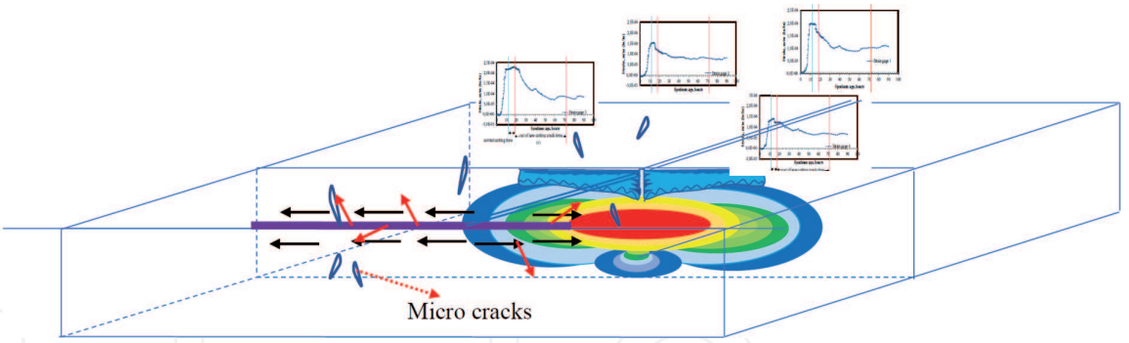

Figure 25.
Bouncy force of microprestress.

condition is marked by the end of ettringite growth. Based on this and **Figure 17**, it begins at around 18 hours of age. Distribution of stresses under the saw cutting is wider to both sides in brittle condition than in plastic condition (**Figure 14c** and **a**). Estimates of stress contours under brittle conditions are presented in **Figure 25**.

The center of the saw cutting line shows the smallest deformation (**Figure 2**), but surrounded by a larger strain (**Figure 25**). It happened at the age of less than 10 hours (**Figure 2**). The stress that causes this strain is withheld by the concrete if there is no room for expansion. Concrete bonds may still be able to withstand these stresses, but by cutting in brittle conditions, the restrained stress increases with a high stress that widens at the bottom end of the cutting. The consequence of this situation is a high-stress accumulation that occurs on both sides of the saw cutting line. As a result of this, accumulation on both sides of the saw cutting line is weak making it more vulnerable to crack.

4.3.2.1 Right position dowel

Concrete is a quasi-brittle material where the fracture process zone (FPZ) in the notch condition can be seen in **Figure 13**. In the FPZ area, microcracks are already present. According to the explanation as mentioned above, great stresses are created on the one side. The friction between the dowel and concrete, which is in a micro-crack condition, does not run smoothly along the dowel because the frictional force partially penetrates the microcrack gap. Some microprestresses are bouncy that can crush the dowels and penetrate microcracks (**Figure 25**).

Because cutting is done too late, the large stresses are looking for a way to release the energy. The move of this energy triggers microcracks to be widened on the weak side and it creates a misalignment crack.

4.3.2.2 Shifting dowel

Asymmetrical conditions of stress occur on both sides due to the dowel shift. There have been weak points at locations outside the saw cutting line (**Figure 24**). As a result, transversal cracks can arise outside the saw cutting line. Condition as mentioned in 4.4.2.1. can also occur. Unbalanced condition between shear force between both the sides of cutting line increases by the spread of large stress at the end of cutting depth and unbalanced bouncy force on both the sides of the cutting line. The unbalanced force leads misalignment cracks to occur on the side of the shift direct dowel.

5. Resume

1. In the concrete pavement, there are microprestress forces, shear forces between dowel and concrete, microprestress resilient forces concerning dowels, shear forces, and tension forces at the base of the concrete pavement.

2. Microprestress is ±7.730003 MPa. The biggest contribution is disjoining pressure and the second is product hydration growth.

3. Disjoining pressure needs to be reduced by maintaining humidity in the concrete pavement at an early age because disjoining pressure will decrease if the water film thickness is large. Although maintaining high humidity makes evaporation also higher, the danger due to evaporation is smaller than the danger of disjoining pressure.

4. Expansion and shrinkage occur in concrete pavement alternately.

5. Free open space is needed to make space for the concrete pavement to expand and shrink and release stress that occurs by saw cutting.

6. Excellent result of cutting time will be obtained at highest inner temperature, which shows high product hydration growth.

7. Raoufi, 2008, illustrates that excellent results of cutting time will be obtained at f_c '800–1000 psi (5.5–6.9 MPa). It is difficult to know the concrete strength (f_c ') at very early age. Compressive strength factor before 1 day has not been found. As a guide, cutting on toll roads in Indonesia is 12–18 hours.

8. If the strength of concrete is smaller than microprestress, microcracks occur in the concrete pavement.

9. Cutting in the window time raises the stress below the tip of the notch that is spread evenly until the base of concrete pavement.

    - Dowel in the right position: no misalignment cracks occur.
    - Dowel shifts: there are imbalance stresses resulting in cracks on the side where the dowel shifts.

10. Cutting late raises the stress below the notch tip and is greater than at the bottom of the concrete pavement. This stress will accumulate with microprestress, shear stress, tensile stress, and resilient stress.

    - Dowel in the right position: this tension will break a weak bond. If one of the bonds breaks because it is unable to withstand the accumulation of the stresses, the stresses will release its energy. Furthermore, the stresses move along the line where a large stress occurs on one side of the cutting line.
    - Dowel shift: an event equal to all of the above description coupled with an unbalanced dowel and concrete shear force creates a misalignment of cracks on one of the weak sides.

11. The implementation of concrete pavement requires the following:

    - Conformity to mix design regarding the amount and quality of material and environment.

    - Designers and managers need to have a good understanding of the consequences of neglect even if it is only one step. The implementation of concrete pavement requires high discipline at each stage. Negligence on one part, because of lack of understanding, and bad discipline or field condition can cause cracks. Any negligence during the construction process may lead to premature distresses in concrete pavement slabs.

6. Conclusion

Saw cutting done during window time causes the stress at the end of the notch to be spread evenly to the bottom of the concrete pavement. In addition to these stresses in concrete pavement, there are microprestress forces, dowels and concrete shear forces, microprestress resilient forces concerning dowels, shear forces, and tension forces at the base of the concrete pavement. Sufficient concrete strength is needed to withstand the accumulation of all these stresses, so saw cutting must be done at an adequate age but still in a condition between plastic and brittle.

The mechanism of the crack misalignment has been studied. The main cause of crack misalignment is that the cutting is done late, that is, after the window cutting time or in brittle conditions. This causes the stress not to be distributed evenly downward but large stresses occur at the lower end of the notch, which spread on both sides of the cutting line. This large stress will break the weak bond and the stress continues to travel along the cutting line because there is a large stress on the cutting line. The consequence of this is that there is a misalignment crack.

Dowel shift causes an imbalance of stress below the notch tip to increase. If the concrete is not able to withstand this imbalance, misalignment cracks arise even though the saw cutting is done at window time. Misalignment cracks tend to appear along the dowel shift.

Every mix concrete has special properties. We are suggested to test the inner temperature in plate sample with the dimension equal to one segment of real concrete pavement. The high inner temperature to be a guide to saw cutting time.

Acknowledgements

My gratitude goes to the Faculty of Engineering, University of Lampung, for supporting this research. I would like to give my highest appreciation to the Faculty of Engineering, University of Indonesia, for locating and maintaining test specimens.

Conflict of interest

"The authors declare no conflict of interest."

IntechOpen

IntechOpen

Author details

Chatarina Niken
Faculty of Engineering, Civil Engineering Department, University of Lampung, Bandar Lampung, Indonesia

*Address all correspondence to: chatarinaniken@yahoo.com

IntechOpen

© 2020 The Author(s). Licensee IntechOpen. This chapter is distributed under the terms of the Creative Commons Attribution License (http://creativecommons.org/licenses/by/3.0), which permits unrestricted use, distribution, and reproduction in any medium, provided the original work is properly cited. CC BY

References

[1] Jagana R, Kumar CV. High-strength concrete. International Journal of Engineering Science & Research. 2017;**6**(2):394-407. DOI: 10.5281/zenodo.291853

[2] Jenning HM, Thomas JJ, Georgios C, Gevrenov JS, Ulm F-J. Nanostructure of CSH Gel in Cement Paste as a Function of Curing Conditions and Relative Humidity. In: Proceeding of the Concreep 7; September 12th. France: Ecole Centrale de Nantes; 2005. p. 7

[3] ACI Committee 360. ACI 360R-06. Design of Slab on Ground. American Concrete Institute; 2006. pp. 1-74. ASIN: B002R0QLVS

[4] Purnawan U. The influence of base course type on rigid pavement concrete strength. In: Proceeding of the 2nd Annual Applied Science and Engineering Conference (AASEC); 24 Agustus 2017; Bandung, Indonesia. IOP Conference Series: Materials Science and Engineering 288 (218). pp. 1-6. DOI: 10.1088/1757-899X/288/1/012120

[5] ACI Committee 209. ACI 209R-92 Prediction of Creep, Shrinkage, and Temperature Effects in Concrete Structure; 2002. pp. 1-47. ISBN: 9780870311222

[6] Al-Jumaili MA. Maintenance and repair of early cracking in airfield apron rigid pavement. Applied Research Journal. 2017;**3**(3):109-113. DOI: http://arjournal.org

[7] Niken C, Siswanto Y, Widodo, Tjahjono E. Cracking of open traffic rigid pavement. In: Proceeding of the SICEST Conference; 28 April 2016; Palembang, Indonesia; 2017. MATEC Web Conference 101, 05009. 2017. pp. 1-6

[8] Fairbain EMR, Azenha. Thermal cracking of massive concrete structure. In: Fairbain EMR, Azenha, editors. Hand Book of RILEM State of the Art Report of the RILEM Technical Committee 254 CMS. Springer. 2019. pp. 1-12. DOI: 10.1007/978-3-319-76617-1

[9] Well SA, Philips BM, Vandenbossche JM. Quantifying built-in construction gradients and early-age slab deformation caused by environmental loads in a jointed plain concrete pavement. International Journal of Pavement Engineering. 2006;**7**(4):275-289. DOI: 10.1080/10298430600798929

[10] Rabbat BG, Russell HG. Friction coefficient of steel on concrete or grout. Journal of Structural Engineering. 1985;**111**(3):505-515. DOI: 10.1061/(ASCE)0733-9445(1985)111:3(505)

[11] Sapountzakis EJ, Katsikadelis JT. Creep and shrinkage effect on the dynamic analysis of reinforced concrete slab-and-beam structures. In: Proceeding of the European Conference on Computational Mechanics; 31 August – 3 September 1999; Munich, Germany. 1999. pp. 1-17 https://www.researchgate.net/publication/280125775

[12] Mehta Y, Ali AW. Field cracking performance of airfield rigid pavements. Journal of Traffic and Transportation Engineering. 2017;**4**(4):380-387. DOI: 10.1016/j.jtte.2017.05.010

[13] Raoufi K, Radlinska A, Nantung T, Weiss J. Practical considerations for determining the time and depth of saw-cuts in concrete pavement. Transportation Research Record Journal of the Transportation Research Board. 2008;**2081**(1):110-117. DOI: 10.3141/2081-12

[14] Pradena M, Houben L. Influence of early-age concrete behavior on concrete pavement performance. Gradevinar. 2016;**69**(9):875-883. DOI: 10.14256/JCE.1931.2016

[15] Ioannides A. Stress prediction for cracking of jointed plain concrete pavements, 1925-2000: An overview. Journal of the Transportation Research Board. 2005;**1919**(1):47-53. DOI: 10.1177/0361198105191900106

[16] Chaddha S, Chauhan AS, Chawla B. A study on the rigid pavement construction, joint and crack formation. International Journal of Modern Trends in Engineering and Research. 2017;**4**(1):138-143. DOI: 10.21884/ijmter

[17] Chen DH, Won M. Field investigations of cracking on concrete pavement. Journal of Performance of Constructed Facilities. 2007;**21**(6):450-458. ISSN (print): 0887-3828, ISSN (online): 1943-5509. https://ascelibrary.org/doi/abs/10.1061/%28ASCE%290887-3828%282007%2921%3A6%28450%29

[18] Kumar B, and Mathur. Early Cracking of Concrete Pavement: Causes and Repair. 2019. Available from: https://www.nbmcw.com/tech-articles/roads-and-pavements/4988-early-cracking-of-concrete-pavement-causes-and-repairs.html

[19] ACI Committee 224. ACI 224R-0.1. Control Cracking of Concrete Structure. American Concrete Institute; 2008. pp. 1-47. ISBN: 978-0-87031-056-0

[20] Buchta V, Janulikova M, Fojtik. Experimental test of reinforced concrete foundation slab. Procedia Engineering. 2015;**114**:530-537. DOI: 10.1016/j.proeng.2015.08.102

[21] ACI Committee 325. ACI 325.12R-02. Guide for Design of Jointed Concrete Pavement for Streets and Local Roads. American Concrete Institute; 2002. pp. 1-32. ISBN: 9780870310768

[22] Slowik V, Schmidt M, Kässler D, Eiserbeck M. Capillary pressure monitoring in plastic concrete for controlling early age shrinkage cracking. Journal of The Transportation Research Board. 2014;**2441**(1):1-5. DOI: 10.3141/2441-01

[23] Kurtis K. Innovations in cement-based materials: Addressing sustainability in structural and infrastructure applications. MRS Bulletin. 2015;**40**(12):1102-1109. DOI: 10.1557/mrs.2015.279

[24] Bažant ZP, Fellow ASCE, Hauggaard AB, Baweja S, Ulm FJ. Microprestress- solidification theory for concrete creep. I: Aging and drying effects. Journal of Engineering Mechanics. 1997:1188-1194. ISSN (print): 0733-9399, ISSN (online): 1943-78. 1997

[25] Craipeau T, Lecompte T, Toussaint F, Perrot. Evolution of concrete/formwork interface in slip forming process. In: Wangler T, Flatt RJ, editors. Book Series of First RILEM International Conference on Concrete and Digital Fabrication- Digital Concrete. Springer International Publishing; 2018. p. 12. https://hal.archives-ouvertes.fr/hal-01881000. Print ISBN: 978-3-319-99518-2, Electronic ISBN: 978-3-319-99519-9

[26] Slowik V, Schmidt M, Friztzsch R. Capillary pressure in fresh cement-based materials and identification of air entry value. Cement and Concrete Composite Journal. 2008;**30**(7):557-565. DOI: 10.1016/j.cemconcomp.2008.03.002

[27] Vanhove Y, Djelal C, Magnin A. A device for studying fresh concrete friction. Cement, Concrete, Aggregate Journal. 2004;**26**(2):35-41. DOI: 10.1520/CCA11897

[28] Holzer L, Gasser P, Muench B. Quantification of capillary pores and hardly grains in cement paste using FIB-Nanotomography. In: Konsta-Gdoutos, Maria S, editors. Hand Book of Measuring, Monitoring and Modeling Concrete Properties. An

International Symposium Dedicated to Professor Surendra P. Shah, Northwestern University, USA. Springer. 2006. pp. 509-516. DOI: 10.1007/978-1-4020-5104-3_62

[29] Danov KD, Ivanov IB, Ananthapadmanabhan KP, Lips A. Disjoining pressure of thin films stabilized by nonionic surfactants. Advances in Colloid and Interface Science Journal. 2006;**128-130**:185-215. DOI: 10.1016/j.cis.2006.11.011

[30] Peng T, Firouzi M, Li Q, Peng K. Surface force at the nanoscale observation of non-monotonic surface tension and disjoining pressure. Physical Chemistry Chemical Physic Journal. 2015;**17**(32):20502-20507. DOI: 10.1039/c5cp03050a